Reaction of $O(^3P)$ with $ClONO_2$: Rate Coefficients and Yield of NO_3 Product

Leah Goldfarb,[†] Matthew H. Harwood,[‡] James B. Burkholder, and A. R. Ravishankara*[,§]

NOAA Aeronomy Laboratory, 325 Broadway, Boulder, Colorado 80303 and Cooperative Institute for Research in Environmental Sciences, University of Colorado, Boulder, Colorado 80309

Received: April 21, 1998; In Final Form: June 29, 1998

The rate coefficient for the reaction $O(^3P)$ with $ClONO_2$, k_1, was measured between 202 and 325 K using two methods: pulsed laser photolysis with time-resolved atomic resonance fluorescence detection of the O atoms and pulsed laser photolysis with long-path tunable diode laser absorption for detection of NO_3 radicals. The measured rate coefficient is summarized by $k_1 = (4.5 \pm 1.4) \times 10^{-12} \exp[(-900 \pm 80)/T]$ cm^3 molecule^{-1} s^{-1}, with $k_1(298\ \text{K}) = (2.2 \pm 0.2) \times 10^{-13}$ cm^3 molecule^{-1} s^{-1}. The yield of NO_3 radical in this reaction was measured to be essentially unity. Our results are compared with those from previous studies.

Introduction

Chlorine nitrate, $ClONO_2$, is a temporary reservoir of chlorine and, to a lesser extent, nitrogen oxides in the stratosphere. It is formed by the reaction of ClO and NO_2 in the presence of a third body. It is removed via photolysis, heterogeneous/multiphase reactions, and free-radical reactions. The rates of these processes determine the partitioning of chlorine and, to some extent, nitrogen oxides between active forms, which can destroy stratospheric O_3, and reservoir forms, which do not. The relative importance of these different processes depends on the location and season. In general, reactions of $ClONO_2$ with free radicals are less important than its loss via photolysis and heterogeneous reactions in the lower stratosphere. One of the free radical reactions of interest is that of $O(^3P)$ with $ClONO_2$:

$$O(^3P) + ClONO_2 \xrightarrow{k_1} \text{products} \quad (1)$$

If $ClONO_2$ were exclusively destroyed in the stratosphere via reaction 1, its lifetime would be on the order of 30 h at 35 km in the midlatitudes ([O] = 1×10^8 cm^{-3}). At lower altitudes, where O-atom concentrations are lower, this reaction is less important relative to photolysis and heterogeneous/multiphase reactions.

Knowledge of k_1, the rate coefficient for reaction 1, is useful for some laboratory studies involving $ClONO_2$ (e.g., see ref 1) as well as in improving the database on the reactivity of $ClONO_2$. Therefore, k_1 was measured as a part of a larger effort in our laboratory[2−7] aimed at understanding the atmospheric chemistry of chlorine nitrate.

The rate coefficient for reaction 1 has been previously reported at 298 K as well as at other temperatures. The currently recommended value[8] for this rate coefficient, based on the studies of Molina et al.,[9] Kurylo,[10] and Adler-Golden and Wiesenfeld,[11] is $k_1(298) = 2.0 \times 10^{-13}$ cm^3 molecule^{-1} s^{-1}, with an uncertainty factor of 1.5 (i.e., it covers the range ($1.3-3.0) \times 10^{-13}$ cm^3 molecule^{-1} s^{-1}). The temperature dependence of k_1, $E/R = 900$ K, is based on the results of Molina et al.[9] and Kurylo,[10] and the quoted uncertainty in this value is $\Delta E/R = 200$ K.

Reaction 1 has many energetically accessible product channels:

$$O(^3P) + ClONO_2 \rightarrow ClO + NO_3\ (-23.1\ \text{kcal mol}^{-1}) \quad (1a)$$

$$\rightarrow ClONO + O_2\ (-62.1\ \text{kcal mol}^{-1}) \quad (1b)$$

$$\rightarrow ClNO_2 + O_2\ (-52.1\ \text{kcal mol}^{-1}) \quad (1c)$$

$$\rightarrow OClO + NO_2\ (-34.6\ \text{kcal mol}^{-1}) \quad (1d)$$

$$\rightarrow ClOO + NO_2\ (-33.9\ \text{kcal mol}^{-1}) \quad (1e)$$

$$\rightarrow ClNO + O_3\ (-28.3\ \text{kcal mol}^{-1}) \quad (1f)$$

$$\rightarrow Cl + NO_2 + O_2\ (-19.1\ \text{kcal mol}^{-1}) \quad (1g)$$

$$\rightarrow ClO + NO + O_2\ (-18.6\ \text{kcal mol}^{-1}) \quad (1h)$$

The enthalpies of the reaction at 298 K, $\Delta H_r°(298\ \text{K})$ are shown in the parentheses. This list includes channels where the products may not adiabatically correlate with the reactants. To our knowledge, only Smith et al.[12] had previously provided some information about the products of reaction 1. They suggested the products to be O_2 and ClONO to explain the end products they observed in the photodissociation of $ClONO_2$. Here, we report the rate coefficient for reaction 1, k_1, as a function of temperature and the yield of the NO_3 product.

Experimental Section

Two apparatus with different detection techniques were used in this study: (1) a pulsed photolysis/atomic resonance fluorescence (PP/RF) apparatus to measure k_1 and (2) a pulsed photolysis long-path UV−vis absorption (PP/LPA) apparatus

[†] Presently at the Laboratory for Atmospheric and Space Physics, University of Colorado, Boulder, CO 80309.

[‡] Currently at Royal Dutch Shell Oil Company, The Netherlands.

[§] Also affiliated with the Department of Chemistry and Biochemistry, University of Colorado, Boulder, CO.

* Address correspondence to NOAA, R/E/AL2, 325 Broadway, Boulder, CO 80303. E-mail: ravi@al.noaa.gov. Fax: 303-497-5822.

10.1021/jp9819386 CCC: $15.00
Published on Web 09/09/1998

to quantify the NO_3 product yield and to measure k_1. For ease of presentation, the two apparatus and experiments are discussed separately.

O-Atom Resonance Fluorescence. In the RF experiments, the temporal profile of $O(^3P)$, hereafter referred to as the O atom, was monitored by vacuum UV atomic resonance fluorescence. This apparatus has been described in detail elsewhere.[13] Only a few essential details are given here. A Pyrex reactor (~150 cm^3) was temperature regulated (± 1 K) by circulating methanol or ethylene glycol through its jacket. A retractable thermocouple inserted into the reaction region, defined by the volume produced by the intersection of the photolysis and probe light beams, was used to measure the temperature of the gases inside the cell.

O atoms were generated by photolyzing O_3 at 308 (XeCl excimer laser) or 532 nm (second harmonic of a Nd:YAG laser) in N_2. Photolysis of O_3 at 308 nm produces both $O(^1D)$ and $O(^3P)$:[8]

$$O_3 + h\nu\ (308\ nm) \rightarrow O(^1D) + O_2\ (^1\Delta) \qquad (2a)$$

$$O_3 + h\nu\ (308\ nm) \rightarrow O(^3P) + O_2\ (^3\Sigma) \qquad (2b)$$

Greater than 99% of $O(^1D)$ was quenched to $O(^3P)$ by 15 Torr of N_2 present in the cell in less than 0.4 μs.

$$O(^1D) + N_2 \rightarrow O(^3P) + N_2 \qquad (3)$$

$k_3(298\ K) = 2.6 \times 10^{-11}$ cm^3 $molecule^{-1}$ s^{-1}.[8] Photolysis of O_3 at 532 nm, in the Chappuis band, leads only to $O(^3P)$:

$$O_3 + h\nu\ (532\ nm) \rightarrow O(^3P) + O_2\ (^3\Sigma) \qquad (2c)$$

It is known that $O_2(^1\Delta)$ reacts with O_3 to produce O atoms.[8] Even if $O_2(^1\Delta)$ was formed in reaction 2c, its contribution to the measured value of k_1 should be negligible since it reacts very slowly with O_3 ($k(298\ K) = 3.8 \times 10^{-15}$ cm^3 $molecule^{-1}$ s^{-1}).[8] To our knowledge, the reaction of $O_2(^1\Delta)$ with $ClONO_2$ has not been studied and has no energetically allowed pathways to produce O atoms.

The fluorescence from the $^3S \rightarrow {}^3P$ transition (130.22−130.60 nm) of the oxygen atom, excited by the resonance lamp, was detected by a solar-blind photomultiplier tube (PMT). A calcium fluoride window mounted in front of the PMT blocked Lyman-α radiation, and the space between this window and the PMT was flushed by nitrogen. The detection sensitivity, as determined by measuring the signal level from a known concentration of O atoms, was $\sim 2 \times 10^9$ atom cm^{-3}. (The detection sensitivity is defined as the O-atom concentration at which the signal divided by the square root of the background for a 1 s integration is unity.) A known concentration of O atoms was generated by photolyzing a measured concentration of O_3 with a laser pulse of known fluence. Approximately 10^3 postphotolysis profiles were co-added to improve the signal-to-noise ratio in the temporal profile measurements. Signals 2 ms prior to the O-atom production were measured to obtain the background-scattered resonance lamp light levels.

The temporal profiles of O atoms were measured in ~50 Torr of He (with at least 15 Torr of N_2) under pseudo-first-order conditions in O atoms (typically $[ClONO_2]/[O]_0 > 1000$, where $[O]_0$ is the initial concentration of O atoms) with the gas mixture flowing through the reaction region at ~20 cm s^{-1}. The gas flow velocity was sufficient to replenish the reaction region with a fresh reaction mixture between photolysis pulses. Before reaching the reactor, the gas mixture passed through two absorption cells in series (a 100 cm cell followed by a 10.6 cm cell). Intensities (I_o) in the absence of $ClONO_2$ and O_3 at 213.9 (first cell) and 253.7 nm (second cell) were first measured. Then ozone was added downstream of the first cell, and its concentration was determined in the 10.6 cm cell by the attenuation of the 253.7 nm light ($\sigma_{O_3}^{253.7} = 1.16 \times 10^{-17}$ cm^2 $molecule^{-1}$). Then, $ClONO_2$ was added upstream of the first cell, and the attenuation of 213.9 nm light was measured to obtain the concentration of $ClONO_2$ ($\sigma_{ClONO_2}^{213.9} = 3.39 \times 10^{-18}$ cm^2 $molecule^{-1}$). Dilution of the O_3 due to the addition of $ClONO_2$ was minimal, and the ozone concentration was essentially unchanged. This negligible change was evident from the measured light intensity at 253.7 nm as $ClONO_2$ was added; it decreased by an amount consistent with that expected from the concentration of $ClONO_2$ flowing through this cell. Note that the exact concentration of O_3 was not needed, since the rate coefficients were measured under pseudo-first-order conditions in O-atom concentrations. The concentrations of both O_3 and $ClONO_2$ were corrected for the temperature and pressure differences between the absorption cells and the reactor. Concentrations of O_3, $O(^3P)$, and $ClONO_2$ were typically 3×10^{14} molecule cm^{-3}, 6×10^{10} atom cm^{-3}, and $(2-18) \times 10^{14}$ molecule cm^{-3}, respectively.

Long-Path Absorption (LPA) Measurements. In the LPA study, the temporal profile of NO_3 was measured by detecting the attenuation of the 662 nm radiation from a tunable diode laser. Only NO_3 contributes significantly to the changes in absorption of 662 nm light in this system after photolysis. The LPA apparatus is the same as that used in our previous study[5] of the reaction of Cl atoms with $ClONO_2$. Therefore, only the aspects of the experiments relevant to the understanding of the present study are discussed here.

The concentrations of $ClONO_2$ and O_3 were measured in the reactor via UV absorption spectroscopy between ~200−350 nm using a 0.27 m spectrometer equipped with a CCD detector. Both $ClONO_2$ and O_3 have relatively unstructured absorption spectra in this wavelength region. Yet by fitting linear combinations of the reference absorption spectra of O_3 and $ClONO_2$ to the spectrum of the cell contents and minimizing the residual, we were able to determine the concentration of both species accurately. Using this method, we also established that, within the error of our measurements (absorbance of ~0.001), no other absorbing species were present in the cell, i.e., all the measured absorption was accounted for by $ClONO_2$ and O_3. The concentrations of O_3 and $ClONO_2$ were also measured in two separate absorption cells, as in the case of the RF experiments. Concentrations determined by the single-wavelength method agreed to within 10% of those measured in the reactor by the CCD. The concentrations of the cell contents were measured both before and after photolysis.

Either the D_2 lamp radiation, to analyze the cell contents by UV absorption, or the 308 nm photolysis laser beam passed through the cell at a given time. Positive position mounts allowed us to quickly and reproducibly switch the beams. The single-wavelength measurements were used to monitor any significant changes in the reactant concentrations during the acquisition of temporal profiles after the D_2 lamp beam was replaced by the laser beam.

The $O(^1D)$ atoms produced by the 308 nm photolysis of O_3 were quickly quenched to O atoms by 200 Torr of N_2 (reaction 3). The 308 nm beam unavoidably photolyzed $ClONO_2$ also. To reduce the contribution of the possible reaction of $ClONO_2$ photolysis products with O atoms while maximizing the loss of O atoms via reaction with $ClONO_2$ (rather than with O_3),

the laser fluence was maintained at <15 mJ pulse^{-1} cm^{-2} and the concentration of $ClONO_2$ was at least 4 times greater than that of O_3.

A beam-combining mirror, which transmitted the 662 nm diode laser beam and reflected the 308 nm photolysis beam into the cell, was used to co-propagate the photolysis and probe laser beams. The 662 nm beam was adjusted to be in the center of the photolysis beam inside the reactor. The diode laser ran single mode with an output power between 3 and 5 mW. The nominal wavelength of the diode laser was measured using a scanning monochromator. The exact wavelength of the laser need not be known because we measured the relative yields; however, it should not change during our experiments to keep the detection sensitivity the same. Therefore, the laser wavelength was locked to 662 nm, the peak of the NO_3 absorption feature, by adjusting the laser current (~50 mA) and temperature (~300 K). Even if there was a small drift (which was much less than 0.1 nm), the absorbance for a given concentration of NO_3 would not change because the absorption cross-section of NO_3 in this region, 662.0 ± 0.1 nm, is essentially constant.

The intensity of the 662 nm beam passing through the reactor prior to the photolysis laser pulse was taken to be I_o. The intensity after the laser pulse, I_t, was used with I_o to calculate the absorbance as a function of time. Thus, we measured only absorption changes due to photolysis. From the absorbance, the concentration of NO_3 at any given time was computed using the known path length (92 cm) and the NO_3 absorption cross-section at 662 nm (2.2×10^{-17} cm^2).[1] The time segments for absorbance measurements varied between a few microseconds and a few milliseconds, depending on the experiments. The calculated sensitivity for NO_3 detection for one laser pulse was ~1×10^{10} molecule cm^{-3} (absorbance of ~2×10^{-5}).

The yield of NO_3 in reaction 1 and the rate constant k_1 were deduced from the same set of NO_3 profiles, which were acquired as follows. Nitrogen carrier gas was flowed through the reactor. A spectrum, I_0, of the cell content was measured using the CCD. O_3 and $ClONO_2$ were added to the N_2 flow from their respective reservoirs, and a second spectrum, I, was recorded. Using the two spectra, the concentrations of O_3 and $ClONO_2$ in the reactor were determined. Necessary mirrors were repositioned to propagate the excimer and diode laser beams through the reactor. The intensity of the diode laser beam exiting the reactor was measured by a photodiode detector. The gas mixture (containing O_3 and $ClONO_2$) was photolyzed by the 308 nm laser beam, and the temporal profile of NO_3 absorption was recorded by monitoring the 662 nm diode laser beam. The NO_3 data acquisition was triggered ~4 ms before the laser pulse to obtain a background signal (I_o). Typically, 5−100 profiles were co-added to enhance the signal-to-noise ratio. The mirrors were repositioned to pass the D_2 lamp beam, and the concentrations of O_3 and $ClONO_2$ were remeasured. O_3 and $ClONO_2$ were replaced by N_2O_5, and its concentration was measured by UV absorption using the CCD, as in the case of $ClONO_2$ and O_3. The mixture was photolyzed by the 308 nm laser pulse, and the temporal profile of NO_3 produced was recorded. Following photolysis, the concentration of N_2O_5 was measured again. While acquiring the temporal profiles, the concentrations of N_2O_5 or O_3 and $ClONO_2$ were monitored via the single-wavelength measurements in absorption cells external to the reactor. The sequence of measurements was repeated at several $ClONO_2$ and N_2O_5 concentrations (4−8) at 298, 273, and 248 K.

Materials. Chlorine nitrate was synthesized[14] by reacting Cl_2O with an excess of N_2O_5 and purified by several trap-to-trap distillations (using three traps at 195, 159, and 78 K). The sample used in the RF study was analyzed by chemical ionization mass spectrometry (CIMS) to quantify the amount of NO_2 (<0.05%), Cl_2 (<0.2%), OClO (0.05%), and Cl_2O (0.1%) impurities. The sample used in the LPA system was analyzed by UV absorption only; the levels of NO_2, Cl_2, OClO, and Cl_2O were <0.05%, <0.5%, 0.5%, and <0.5%, respectively. The samples were used without further purification. Chlorine nitrate was stored in the dark at 195 K. N_2O_5 was synthesized by reacting O_3 with NO_2. N_2O_5 emerging from the end was trapped in a vessel held at 195 K. The NO_2 was made via the reaction of O_2 with purified NO (higher nitrogen oxides were removed by passing NO through a silica-gel trap at 195 K). The N_2O_5, stored in a glass trap at 195 K, was eluted by a flow of N_2. The He carrier gas used in the RF study was dried by flowing it through a molecular-sieve trap held at liquid nitrogen temperature. Mixtures of ozone in the diluent gas were prepared in 12 L bulbs and used in the RF experiments. For the LPA experiments, ozone was eluted by passing dried N_2 through a silica-gel trap at 195 K that stored ozone. Such a procedure was necessary to maintain a steady high O_3 concentration at the flow velocities and pressure used in this experiment. Helium (UHP >99.999%) and N_2 (UHP >99.9995%) were used as supplied. The N_2 gas used for the flush between the reactor and the PMT was 99.98% pure.

Results

The data acquisition and analysis for the RF and long-path absorption experiments were different and are presented in separate sections below.

O-Atom Resonance Fluorescence. The temporal profile of O atoms in the presence of $ClONO_2$ following their photolytic production from O_3 was governed by the following reactions:

$$O(^3P) + ClONO_2 \rightarrow \text{products} \quad (1)$$

$$O(^3P) \rightarrow \text{products} \quad (4)$$

$$O(^3P) \rightarrow \text{loss} \quad (5)$$

Reactions 4 and 5 represent O-atom loss out of the reaction zone via processes other than reaction 1 and are assumed to be first order in O-atom concentration. Reaction 4 represents reactions of O atoms with O_3 and any impurities in the gas mixture or species created by the laser photolysis; these reactions are assumed to be first order in O atoms. Orkin et al.[15] have discussed how one could explicitly deal with the loss of O atoms via a combination of diffusion and reaction. In our experiments, since the loss of O atoms in the absence of $ClONO_2$ was essentially exponential, we simply treated this loss as a first-order process. The O-atom temporal profiles due to the above process were governed by a simple exponential decay given by

$$\ln(S_t) = \ln(S_o) - k't \quad (6)$$

where S_t and S_0 are the RF signals of O atoms at time t and 0, respectively, and

$$k' = k_1[ClONO_2] + k_5 + k_{4a}[O_3] + \sum_i k_{4i}[\text{impurity } i] \quad (7)$$

In the above expression, the contribution to the O-atom loss via reaction with O_3 is denoted by $k_{4a}[O_3]$, while the contribution due to impurities is represented by the last term in eq 7. A typical O-atom temporal profile is shown in Figure 1. The line

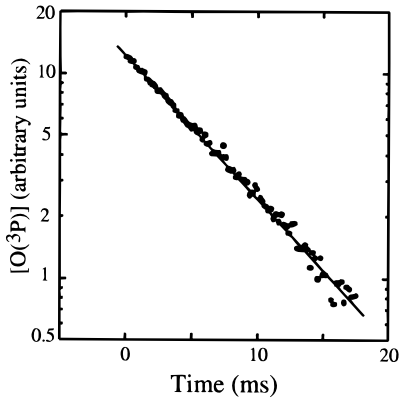

Figure 1. Temporal profile of the O-atom signal in the presence of 4 $\times$ 10^{14} molecule cm^{-3} of $ClONO_2$ at 299 K. The line is a fit of the data to eq 6.

in the figure is the linear least-squares fit of the data to eq 6. Values of k' were measured at various concentrations of $ClONO_2$ (shown in Table 1) to obtain k_1 from plots of k' versus $[ClONO_2]$ using a weighted linear least-squares fit of the data to eq 7. A typical plot for k' versus $[ClONO_2]$ at 298 K and the linear least-squares line are shown in Figure 2. The second-order rate constant k_1 was measured at l0 temperatures between 202 and 325 K.

Table 1 lists the experimental conditions and the measured values of k_1 along with the obtained precision in the plots of k' versus $[ClONO_2]$. The obtained values of k_1 are plotted in the Arrhenius form in Figure 3.

The fluence of the 532 nm beam was varied over a factor of 3 (20.5−64.8 mJ cm^{-2} $pulse^{-1}$). The measured value of k_1 was independent of laser fluence, and hence, the photoproducts of $ClONO_2$ could not have contributed significantly to the measured value of k_1. As noted earlier, the expected concentrations of the products of photodissociation of $ClONO_2$ are so small ($<10^{11}$ cm^{-3}) that they cannot contribute significantly to the measured O-atom loss-rate coefficients. The flow rate was varied by a factor of 4 (20−80 cm s^{-1}), and the pressure was changed from 40 to 60 Torr. These experimental conditions were varied to test for systematic errors that could have affected the kinetic determination. The measured rate coefficients were invariant for the above changes, within the precision of the measurements.

Long-Path Absorption Measurements. Since both $ClONO_2$ and O_3 are photolyzed at 308 nm, the obtained NO_3 profiles had contributions from three sources:

$$ClONO_2 + h\nu\ (308\ nm) \rightarrow Cl + NO_3 \qquad (8)$$

$$Cl + ClONO_2 \rightarrow Cl_2 + NO_3 \qquad (9)$$

$$O(^3P) + ClONO_2 \rightarrow NO_3 + ClO \qquad (1a)$$

Photolytic production of NO_3 from reaction 8 was essentially instantaneous. We saw no evidence for the formation of vibrationally excited NO_3 and its subsequent relaxation to the detected ground state on the time scale of our experiments.[5,6] Recent work[7,6,16,17] has shown that the quantum yield for NO_3 and Cl is 0.65 at 308 nm, and the O-atom yield is <0.05. The rate constant for reaction 9 is $\sim$60 times larger than that for reaction 1, such that Cl atoms are removed very rapidly compared to the O atoms. The Cl-atom loss rate is further enhanced in our experiments due to its reaction with O_3. The typical lifetime ($1/e$) for loss of Cl via reactions with $ClONO_2$ and O_3 was <0.25 ms in our experiments. On the other hand, the lifetime for loss of O atoms via reaction 1 was >3 ms. Thus, the contribution of reaction 9 to the measured NO_3 profile was limited to very short times. The NO_3 absorption profile, Figure 4, shows these time scales.

The NO_3 absorbance profiles after $\sim$0.3 ms followed the equation:

$$\ln(A_\infty - A_t) = -k't + \ln(A_\infty - A_0) \qquad (10)$$

where A_∞ is the absorbance after reaction 1 has gone to completion ($t > 0.01$ s), A_t is the time-dependent absorbance, A_0 is the absorbance by NO_3 after photolysis when reaction 9 has gone to completion, and k' is the pseudo-first-order rate constant for the loss of O atoms via reactions 1, 4, and 5. Because the loss of NO_3 was very slow on the time scale for the completion of reaction 1, A_∞ was essentially the same as the maximum absorption that was measured. (We actually accounted for the slow loss of NO_3 in the data analysis.) An example of the temporal profile of $(A_\infty - A_t)$ is shown as the inset in Figure 4. A least-squares fit of this profile yielded k', the first-order rate coefficient for the loss of O atoms. The fit was limited to times after reaction 9 had gone to $>99\%$ completion. In these experiments, loss of O atoms via process 5 is negligibly small and reaction 4 was minimized. The decays extended over 2−3 lifetimes for the O atom and were strictly exponential. The measured values of k' were plotted against the $[ClONO_2]$ to obtain k_1 as the slope. The values of the rate coefficients obtained from the LPA experiments at 298, 273, and 248 K are included in Table 1.

A determination of the NO_3 yield from reaction 1 required the knowledge of three quantities: (i) the initial concentration of O atoms produced, (ii) the fraction of O atoms lost via reaction with $ClONO_2$ (as opposed to other reactions), and (iii) the concentration of NO_3 that was generated from reaction 1a. If NO_3 was produced by reactions other than 1a, such reactions needed to be quantified and/or minimized. Of all these parameters, the initial O-atom concentration is the most difficult to obtain accurately. The O-atom concentration in our experiments was calculated from the measured concentration of O_3 (O-atom precursor), the known O_3 absorption cross-section at 308 nm, and the photolysis laser fluence by assuming the quantum yield for O-atom production in O_3 photolysis to be unity. The laser fluence was deduced from the NO_3 generated by the photolysis of $ClONO_2$ itself or of N_2O_5 in a separate experiment. $ClONO_2$ photolysis generates NO_3, and hence, the laser fluence could be derived from this NO_3 formation since the quantum yield for its formation is known. Therefore, NO_3 from $ClONO_2$ photolysis acted as an "internal fluence calibration".

The NO_3 temporal profiles measured after the photolysis of a mixture of O_3 and $ClONO_2$, such as that shown in Figure 4, were analyzed for NO_3 yield. The absorbance of NO_3 from reaction 1 was separated from that due to $ClONO_2$ photolysis (reaction 8), which is instantaneous on the time scale of our experiments, and reaction 9, which is complete after $\sim$0.25 ms. The concentration of NO_3 generated due to reaction 1, denoted in Figure 4 by M, is clearly seen in the figure as the slowly rising signal which reached a maximum. The value of M, $A_\infty - A_0$, was obtained from the intercept, $\ln(A_\infty - A_0)$, in a plot of $\ln(A_\infty - A_t)$ versus time (inset in Figure 4) using a linear least-squares analysis. This method of obtaining the concentration of NO_3 produced in reaction 1 is referred to here as the graphical method. The concentration of NO_3 generated from

TABLE 1: Measured Values of k_1 (in 10^{-14} cm^3 molecule^{-1} s^{-1}) and Experimental Conditions from Resonance Fluorescence and Long-Path Systems[a]

T, K	$[O]_0$[b]	$[ClONO_2]$[c]	$k_1 \pm (2\sigma$ precision)	% error due to impurities[d]			total uncertainty in %[f]	$k_1 \pm (2\sigma)$[e]
				NO_2	Cl_2O	OClO		
202	6	1.95−19.3	5.49 ± 0.20	10.7	3.56	0.02	12.9	5.49 ± 0.71
206	4	1.26−10.5	5.7 ± 1.1[g]	10.4	3.68	0.02	23.1	5.7 ± 1.3
223	7	0.82−17.3	8.04 ± 0.40	7.0	3.13	0.02	10.4	8.04 ± 0.83
247	5	4.02−17.0	10.6 ± 0.71	5.0	2.98	0.02	10.1	10.6 ± 1.1
248	6	2.82−28.2	10.1 ± 0.92	5.2	3.15	0.02	11.9	10.1 ± 1.2
248	20	9.21−23.5	9.9 ± 1.5[h]	5.3	3.22	0.03	17.1	9.9 ± 1.7
249	6	0.90−13.9	11.0 ± 0.3	4.8	2.92	0.02	8.0	11.0 ± 0.9
249	5	0.84−12.9	10.6 ± 0.7[i]	5.0	3.03	0.02	10.1	10.6 ± 1.1
260	7	0.87−12.0	14 ± 1	3.7	2.51	0.02	9.8	14 ± 1
273	6	0.87−12.5	14 ± 1	3.6	2.77	0.03	9.8	14 ± 1
273	85	8.64−19.2	15 ± 3[h]	3.4	2.58	0.02	21.1	15 ± 3
274	2	2.95−29.0	14.4 ± 0.9	3.5	2.71	0.03	9.2	14.4 ± 1.3
298	770	2.57−11.89	24.9 ± 0.9[g]	1.9	1.83	0.02	6.7	24.9 ± 1.7
298	185	3.47−35.93	21.5 ± 1.0[j,k]	2.3	2.17	0.02	7.6	21.5 ± 1.6
298	77	4.75−19.54	20.3 ± 0.8[j,k,l]	2.4	2.25	0.02	7.2	20.3 ± 1.4
298	21	3.26−16.14	22.7 ± 1.5[j,k,m]	2.2	2.07	0.02	7.4	22.7 ± 1.6
298	54	21.9−83.6	19.1 ± 2.1[h]	2.6	2.40	0.03	12.2	19.1 ± 2.3
298	70	4.21−21.4	22.7 ± 1.5[h]	2.1	1.98	0.02	26.7	22.7 ± 1.7
299	35	2.34−27.0	20.5 ± 0.9[n]	2.4	2.24	0.02	7.4	20.5 ± 1.52
299	13	2.8−30.2	22.7 ± 0.7[o]	2.1	2.02	0.02	6.6	22.7 ± 1.49
⟨298⟩			21.8 ± 0.4					21.8 ± 2.0
325	4	0.72−9.06	28.7 ± 0.7	1.6	1.82	0.02	8.9	28.7 ± 2.6
341	2	0.76−7.46	45 ± 2[p]	1.0	1.27	0.02	13.0	45 ± 5.8

[a] Unless noted, all data are from the RF experiments with the 532 nm photolysis of $\sim 3 \times 10^{14}$ cm^{-3} of O_3 to produce O atoms. [b] In units of 10^{10} cm^{-3}. [c] In units of 10^{14} cm^{-3}. [d] These are upper limits for the contributions. [e] Added 5% uncertainty due to the uncertainty in $ClONO_2$ cross-section at 213.9 nm. Additional uncertainties of 1% and 11% are added to the rate coefficients at 325 and 341 K, respectively, due to the thermal decomposition of $ClONO_2$ and the production of NO_2. All the uncertainties were added in quadrature. [f] Errors are 2σ and include estimated systematic errors. [g] Flow rate increased by a factor of 4. [h] Data from long-path system (photolysis at 308 nm). [i] Laser fluence increased from 32 to 85 mJ cm^{-2} pulse^{-1}. [j] 308 nm photolysis. [k] Laser fluence decreased from 11 to 3.2 mJ cm^{-2} pulse^{-1}. [l] Ozone concentration reduced from 2.3×10^{15} to 7.7×10^{14} molecule cm^{-3}. [m] Ozone concentration lowered to 2.0×10^{14} molecule cm^{-3}. [n] Laser fluence = 47 mJ cm^{-2} pulse^{-1}. [o] Laser fluence = 19 mJ cm^{-2} pulse^{-1}. [p] Thermal decomposition affected the measurement. This value was not included in our calculation of the Arrhenius parameters.

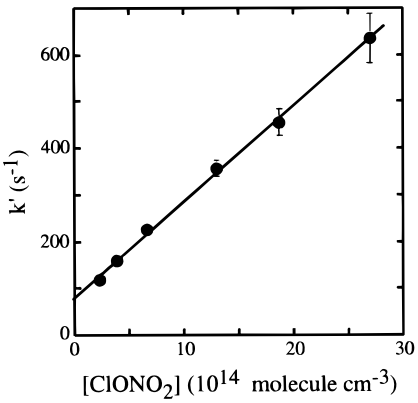

Figure 2. Typical plot of k' vs $[ClONO_2]$ at 299 K. The line through the data is the linear-least-squares fit which yields $k_1 = 2.05 \times 10^{-13}$ cm^3 molecule^{-1} s^{-1}.

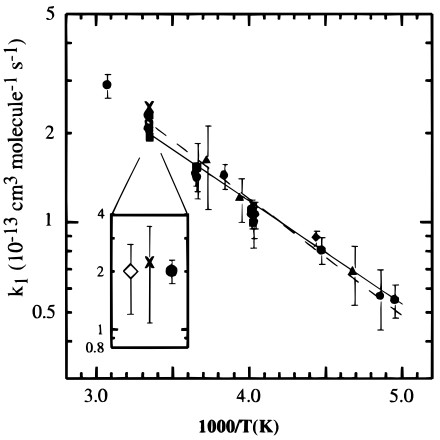

Figure 3. Plot of k_1 as a function of temperature in the Arrhenius form. Work from this laboratory are 532 nm photolysis and RF detection of the O atom (●); 308 nm photolysis and RF detection (○); and 308 nm photolysis and long-path absorption detection of NO_3 (■). Also included in this plot are the findings of Molina et al.[9] (◇), Adler-Golden and Wiesenfeld[11] (×, room temperature only), Kurylo[10] (◆), NASA-JPL recommendation[8] (—), and the fit to our data (- - -). The inset shows the room-temperature values, displaced from each other for clarity. Our value is denoted by the filled circle.

reaction 1, $[NO_3]_{Rx1}$, is given by

$$[NO_3]_{Rx1} = \frac{A_\infty - A_0}{L\sigma_{NO_3}^{662nm}} \qquad (11)$$

where L is the path length through the reactor and $\sigma_{NO_3}^{662nm}$ is the absorption cross-section of NO_3 at 662 nm. The NO_3 yield in reaction 1 was obtained by comparing $[NO_3]_{Rx1}$ with the concentration of NO_3 produced via $ClONO_2$ photolysis and the reaction of Cl atoms with $ClONO_2$, shown in Figure 4 as N. NO_3 is produced from reaction 9 on a very short time scale and is essentially inseparable in our experiments from reaction 8. The quantum yield of NO_3 from the photolysis of $ClONO_2$ at 308 nm[7,6] was taken to be 0.65. A fraction of the Cl atoms generated from $ClONO_2$ reacts with O_3 in our experiments, and this fraction was calculated using known rate coefficients for the Cl-atom reactions with $ClONO_2$ and O_3.[8] This fraction was usually less than 30%, except in some experiments where it was increased to nearly 70% (see Discussion). Such analyses of 14 measurements at 298 K yielded an average value of 0.96 ± 0.17 and are listed in Table 2.

Alternatively, the entire temporal profile was fit to a reaction scheme comprised of reactions 1, 8, and 9, as well as the reaction of Cl with ozone. A commercial computer code, FACSIMILE,[18] was employed to carry out such fits. For each profile, the initial concentration of $ClONO_2$ and O_3 were fixed

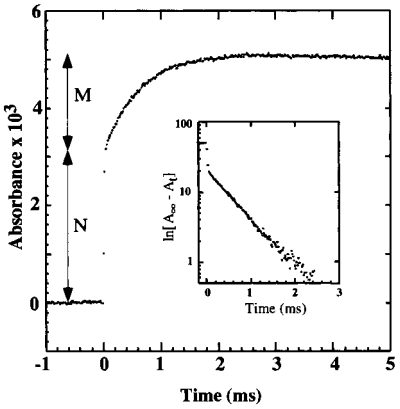

Figure 4. Temporal profile of the NO_3 absorbance following photolysis at 308 nm of a O_3 and $ClONO_2$ mixture ($T = 298$ K). The values of A_∞, the amount arising from reaction 1 (M), and the amount from reactions 8 and 9 (N) are also shown. The inset shows a plot of $(A_\infty - A_t)$, on a log scale, as a function of time. A least-squares analysis of this data yielded k' as the slope and $(A_\infty - A_0)$ as the intercept. The slope was used to derive k_1 and the intercept to obtain the yield of NO_3 in reaction 1; see text for details.

at the values measured. The NO_3 radical concentration produced upon photolysis, $[NO_3]_{phot}$, was a variable in the fitting routine. The $[NO_3]_{phot}$ value obtained by the fit and attributed to the sum of reactions 8 and 9 was used to calculate the initial concentrations of O atoms, $[O]_o$, and the other photolytically produced radicals. The rate coefficient for the loss of NO_3 was assumed to be first order in NO_3 and was a variable in the model. The calculated NO_3 yield from reaction 1 was relatively insensitive (±10%) to changing the assigned rate coefficient for reaction 9 and the initial estimates for the three variables in the model by factors of two. The obtained results are also shown in Table 2 within parentheses.

The measured $[NO_3]_{Rx1}$, calculated from extrapolation of the temporal profiles described earlier, was also compared with $[NO_3]_{Rx12}$, the concentration of NO_3 produced by the photolysis of a known concentration of N_2O_5 at 308 nm.

$$N_2O_5 + h\nu(308\text{ nm}) \rightarrow NO_2 + NO_3 \qquad (12)$$

These N_2O_5 photolyses were carried out before and after photolyzing $ClONO_2/O_3$ mixtures, without changing the laser fluence. The temporal profiles of NO_3 from N_2O_5 photolysis displayed an initial jump due to its photolytic production followed by a slow decay due to loss via reactions with impurities, such as NO_2, and a very slow diffusive loss out of the probe beam area. The NO_3 yield in reaction 1 was calculated using

$$\Phi_{rxn} = \frac{[NO_3]_{Rx1}\sigma_{N_2O_5}[N_2O_5]\Phi_{N_2O_5}}{[NO_3]_{Rx12}\sigma_{O_3}[O_3]} \qquad (13)$$

where $[NO_3]_{Rx1}$ was obtained from the graphical analyses. The absorption cross-sections of O_3 and N_2O_5 evaluated at 308 nm[19,20] are 1.34×10^{-19} and 2.46×10^{-20} cm^2 molecule^{-1}, respectively. The quantum yield for NO_3 from the photolysis of N_2O_5 at 308 nm was taken to be 0.96 ± 0.15.[21]

Discussion

The measured values of k_1 from the LPA method agrees with those from the RF method within the precision of the measurements (Figure 3). In the RF method, the disappearance of the reactant O atom was monitored, and in the LPA method, the appearance of the NO_3 product was measured. In both methods, $ClONO_2$ was much more abundant than O atoms.

Potential sources of errors in the values of k_1 measured in the RF system were (a) loss of O atoms via reaction with species other than $ClONO_2$, such as photoproducts and impurities in the $ClONO_2$ sample, (b) errors in determining the $ClONO_2$ concentration in the reactor, (c) precision of the measured temporal profiles, and (d) thermal decomposition of $ClONO_2$, which leads to reactive impurities as well as a depletion of $ClONO_2$. The loss in $ClONO_2$ due to thermal decomposition and the consequent lowering of the measured value of k_1 is quite small and was always less than a couple of percent. Yet thermal decomposition can be a major problem because it produces species, such NO_2, that can react much faster with O atoms than $ClONO_2$. These errors are discussed below.

In past kinetic studies,[9−11,17,22] short wavelength photolysis (≤308 nm) of various photolytes has been used to produce O atoms. However, $ClONO_2$ absorbs quite strongly at these wavelengths (the absorption cross-section of $ClONO_2$ at 308.15 nm is 1.81×10^{-20} cm^2 molecule^{-1}) and increases further at shorter wavelengths.[2] To minimize $ClONO_2$ photolysis, we employed 532 nm photolysis of O_3 to produce O atoms. At this wavelength, the absorption cross-section of $ClONO_2$ ($\ll 10^{-21}$ cm^2 molecule^{-1}) is so small that only a very small fraction of $ClONO_2$ is photolyzed. In a few experiments, O_3 was also photolyzed at 308 nm to simulate previous studies that utilized shorter wavelength photolysis for O-atom production. These 308 nm photolysis measurements also served to measure k_1 in the RF system under conditions similar to those used in the LPA system to measure the NO_3 yield. At this wavelength, $ClONO_2$ photolyzes to give Cl, NO_3, ClO, and NO_2.[7] Cl atoms react rapidly with $ClONO_2$ to produce Cl_2 and NO_3. The rate coefficients for the reactions of O atoms with ClO, NO_2, and NO_3[8] and the quantum yields for various photoproducts in $ClONO_2$ photolysis at 308 nm are known. Using this information, we calculate the maximum contribution to the removal of O atoms by the reaction of the photoproducts to be <0.6%. To confirm this negligible contribution, the fluence at 308 nm was varied by a factor of 3 (3.2−11 mJ cm^{-2} pulse^{-1}), and the measured values of k_1 did not change. Further, the obtained values agree well with those measured using 532 nm photolysis of O_3. Therefore, we are confident that our measured values of k_1 were not influenced by reactions of photoproducts.

NO_2 is an impurity in our chlorine nitrate samples, and it reacts rapidly with O atoms ($k_{14} = 6.5 \times 10^{-12} \exp(120/T)$ cm^3 molecule^{-1} s^{-1}).[8]

$$O + NO_2 \rightarrow \text{products} \qquad (14)$$

The contribution of this reaction to the measured O-atom profiles increases at lower temperatures where k_1 decreases while k_{14} remains nearly constant. NO_2 in our samples was not detectable via CIMS, as noted earlier. If we assume that NO_2 was present at the concentration given by the upper limits, its contribution to the measured values of k_1 would be <3% at room temperature and <12% at 202 K, the lowest temperature of this study. The contribution of OClO to the loss-rate coefficients of the O atoms was <1% at all temperatures. Cl_2O was the only other impurity that could have reacted with O atoms.

$$O + Cl_2O \rightarrow \text{products} \qquad (15)$$

The rate coefficient for this reaction is $k_{15} = 2.7 \times 10^{-11} \exp(-530/T)$ cm^3 molecule^{-1} s^{-1}.[8] At the lowest temperature examined, reaction 15 contributed <5% to the measured value

TABLE 2: Summary of NO_3 Yield Data from the Long-Path UV−Vis Absorption System

					method of analysis[b]	
T (K)	no. of exp	$[ClONO_2]$[a]	$[O_3]$[a]	$[ClONO_2]/[O_3]$	internal calibration[c]	external calibration
298	14	4.21−83.6	2.94−11.8	0.5−6.5	0.96 ± 0.17 (0.93 ± 0.16)	1.13 ± 0.36
273	5	8.64−19.2	7.47−11.9	1.1−2.2	0.80 ± 0.23 (0.89 ± 0.14)	1.22 ± 0.09
248	4	9.21−23.5	3.87−4.74	1.0−5.4	0.87 ± 0.10 (0.85 ± 0.06)	1.00 ± 0.11

[a] 10^{14} molecule cm^{-3}. [b] The errors are two standard deviations of the mean of the number of measurements shown in column 2. [c] The numbers in parentheses were derived by numerical simulations (see text for details).

of k_1 in the RF study and at most 15% in the LPA work. Since we did not definitely measure these impurities, we did not correct our measured values of k_1. Instead, we have included these maximum potential contributions as uncertainties in reporting our values of k_1 by assuming that the presence of these impurities is uncorrelated. Strictly, the rate coefficients would only be lowered by the presence of these impurities and the error bars should be asymmetric. However, for the sake of simplicity, we have chosen to use symmetric error bounds. The systematic uncertainties due to the presence of the impurities are included in the errors quoted in the last column of Table 1. The specific contribution due to various sources and the derivation of the total uncertainties are also given in the table.

The measured concentrations of $ClONO_2$ are uncertain due to the uncertainties in the path length, the pressures in the reactor and the absorption cell (which was varied to check for decomposition or three-body reactions), and the UV absorption cross-sections of $ClONO_2$ and O_3. We evaluated these uncertainties in a previous study[1] and concluded that they add a systematic uncertainty of <5%, almost completely due to the uncertainty in the absorption cross-section of $ClONO_2$. By measuring the concentration of $ClONO_2$ via absorption in the gas flowing through a cell held at 298 K, we were able to accurately determine its concentration in the reactor, and the absorption cross-section at other temperatures was not needed.

Chlorine nitrate thermally dissociates to produce ClO and NO_2. ClO will either recombine with NO_2 or will react with itself to yield Cl_2 and O_2. Neither Cl_2 nor O_2 reacts rapidly with O atoms under our conditions. However, NO_2 reacts with O atoms rapidly enough (reaction 14) that, if present in significant concentrations, it enhances the measured values of k_1. To check for possible gas-phase or heterogeneous decomposition of $ClONO_2$, the gas flow rate was varied by a factor of 4; k_1 was invariant with the changes in the flow rate for $T \leq 325$ K. Note, if $ClONO_2$ is lost via hydrolysis on the surface, the HNO_3 and HOCl products would not react very rapidly with O atoms.[8] We calculate that for $T \leq 325$, the extent of thermal dissociation of $ClONO_2$ for a typical residence time (∼24 s) in the manifold and photolysis cell was <0.3%. Assuming this upper limit for the thermal dissociation could introduce an error of 11% to k_1 at 325 K; it is negligible at 298 K and below. This uncertainty is included in the errors shown in the last column of Table 1.

At 341 K we saw clear evidence for the thermal decomposition of $ClONO_2$. Even though the extent of thermal dissociation of $ClONO_2$ is calculated to be only 1.5% at 341 K, the measured rate constant was ∼45% higher than that expected from an extrapolation of data assuming an Arrhenius behavior in k_1. The measured higher rate coefficient at 341 K is consistent with the estimated contribution due to NO_2 produced by thermal decomposition. Therefore, the Arrhenius expression given in Table 3 was calculated using data at $T \leq 325$ K. Thermal decomposition was also seen in our study of the Cl + $ClONO_2$ reaction. However, because the Cl atom reacts with NO_2 much slower than with $ClONO_2$, the effects of thermal decomposition manifested itself as a decrease in the measured value of k_{11}.[1]

TABLE 3: Comparison of k_1 (in 10^{-13} cm^3 $molecule^{-1}$ s^{-1}) Measured in This Study with Those from Previous Studies and Recommendations[a]

ref	A[b]	$E/R \pm \Delta E/R$ (K)	k_1(298 K)[b]	f(298 K)	T range (K)
this work	4.5 ± 1.4[c]	900 ± 80	2.20 ± 0.20		202−325
this work	4.5	900 ± 100	2.2	1.15	
11			2.3 ± 1.2		298
9	3.4 ± 0.6	840 ± 60	2.0 ± 0.8		213−295
10	1.87 ± 1.29	692 ± 167	*d*		225−273
	3.03 ± 1.56	808 ± 133			213−295
8	2.9	800 ± 200	2.0	1.5	200−300
25	3.0	808 ± 200	2.0	1.5	213−295

[a] Quoted errors are 2σ from the authors. [b] Our quoted errors include estimated systematic errors in our measurements. [c] The noted error in A is derived by linear least-squares fitting of $\ln(k)$ with $1/T$; $\sigma_A = A\sigma_{\ln A}$. The A value from our measurements has been adjusted to reproduce k(298 K). [d] Kurylo did not measure k_1(298 K) but determined the Arrhenius parameters by measuring k_1 between 225 and 273 K.

Table 3 and Figure 3 show our results along with those from previous studies of k_1. Our results from the LPA experiments agree with those from the RF method, within the uncertainty of the measurements. It is also clear that our results are extremely close to those from studies used to derive the recommended values. Since our data agrees reasonably well with the recently recommended values, we need not restate the possible reasons for the discrepancies with the earlier data. It should be noted that in-situ measurement of the $ClONO_2$ concentration and quantification of the impurities are critical to obtaining an accurate value of k_1. Early measurements of k_1, for example that of Ravishankara et al.,[23] were likely hampered by problems associated with handling and quantifying $ClONO_2$ as well as the reactive impurities.

In Table 3, we have also listed our results in the format used by the recommendations. Combining the results of Molina et al. and Kurylo with our data leads to essentially the same value as that derived from our data alone. It is clear that because of our extensive measurements, the uncertainty in the value of k_1 has been significantly reduced. The larger range of temperatures in this study has helped in reducing the uncertainty in the activation energy for the reaction.

Comparison of reaction 1 with other reactions of O atoms with inorganic chlorinated compounds, Cl_2, ClBr, or Cl_2O, leading to the formation of ClO shows a rough trend with the exothermicity of the reaction. The rate coefficient for the reaction of O atoms with Cl_2O ($\Delta H_r°(298\ K) = -30$ kcal mol^{-1}) is 10 times larger than k_1 at 298 K. The rate coefficient for the reaction of O atoms with Cl_2 ($\Delta H_r°(298\ K) = -6.3$ kcal mol^{-1}) is roughly 10 times smaller than k_1. These large changes are mostly due to the decreasing activation energy with the increasing exothermicity of the reactions.

The NO_3 produced in the reaction can arise from pathways other than reaction 1a. Our method was incapable of directly distinguishing NO_3 production from reaction 1a from that produced via channel 1e, which leads to Cl via the rapid thermal decomposition of ClOO,[24,8] or 1g followed by the reaction of Cl atoms with $ClONO_2$. Cl-atoms react very rapidly with

$ClONO_2$ via reaction 9 such that the rate-limiting step for NO_3 formation will be reaction 1. Thus, the measured temporal profiles of NO_3 cannot help distinguish reaction 1a from reactions 1e and 1g. We indirectly gauged the contribution of these two channels by varying the ratio of $[O_3]$ to $[ClONO_2]$. In this way, the fraction of Cl atoms that reacts with O_3, rather than with $ClONO_2$, will change and alters NO_3 production. Changing the $[ClONO_2]/[O_3]$ ratio by a factor of ~10 at 298 K (~2 at 273 K and ~5 at 248 K), thus changing the fraction of Cl atoms that reacted with O_3 from ~15% to ~65% at 298 K (~30 to ~50% at 273 K and ~20 to 50%), did not appreciably affect the measured NO_3 yield. Given the large uncertainty in the values of the yield, we can say that the sum of the branching ratio for channels 1e and 1g is not very large (<0.3). However, it appears channels 1e and 1g are less likely than channel 1a because the measured rate constant and its variation with temperature are consistent with that for a simple abstraction reaction.

To our knowledge, the yield of NO_3 in reaction 1 has not been measured previously. Our measured yield of NO_3 at 298 K was approximately unity. An average of the values shown in Table 2 would be 1.07 ± 0.36, by taking an average of the internal and external calibration results. The agreement between the values obtained using $ClONO_2$ photolysis as the internal standard and N_2O_5 photolysis as the external standard is good considering the errors involved. On the basis of these measurements, it appears that NO_3 and ClO are the primary products of this reaction and account for at least 70% of the reaction. Obviously, we cannot rule out other minor products.

Smith et al.[12] hypothesized that reaction 1 produced O_2 and ClONO to account for the production of Cl_2, O_2, and N_2O_5 in the 302.5 nm photolysis of $ClONO_2$. They suggested that the photolysis of $ClONO_2$ produced O atoms and that the subsequent reactions of the O atoms led to these products. However, we now know that the quantum yield for the production of O atoms in the photolysis of $ClONO_2$ around 300 nm is <10% and that the major products are $Cl + NO_3$ and $ClO + NO_2$, with the former set being the major products.[7,6,16,17] The subsequent reactions of Cl with $ClONO_2$ and the reaction of NO_3 with NO_2 (either generated by photolysis or decomposition of $ClONO_2$) would lead to the products observed by Smith et al. In the absence of the details of the experiments of Smith et al., it is difficult to say if their observed products could be quantitatively accounted for by the photochemistry in $ClONO_2$ around 300 nm that is now reasonably well understood. However, it is clear that generation of ClO and NO_3 from reaction 1 is not contrary to the end products observed by Smith et al.

It appears that the yield of NO_3 is the same at the three temperatures examined here. The invariance of the yield with temperature suggests that a majority of the reaction proceeds via abstraction and that ClO and NO_3 are the major products.

The intercepts in the plots of the first-order rate coefficients for the loss of O atoms, measured by observing NO_3 production, versus $[ClONO_2]$ were too large (~50−350 s^{-1}) to be accounted for by the known loss processes for O atoms in the absence of $ClONO_2$. This intercept cannot be measured directly, i.e., in the absence of $ClONO_2$. Reactions such as 14 and 15 cannot account for the observed intercepts. If oxygen atoms were reacting with one or more products of reaction 1, such as NO_3, a larger intercept might be observed. However, on the basis of the calculated concentrations of the photoproducts, it appears that secondary reactions were not the cause of this large intercept. Another possibility for the larger intercept is the presence of small amounts of reactive species, such as NO_2, in the main flow of N_2. NO_2 is known to permeate into Teflon. Therefore, to check for this, pure N_2 was used and all the Teflon tubing was replaced by glass; the intercept did not change. Thus, we are at a loss to explain this larger intercept. Yet the agreement between the values of k_1 measured in the LPA apparatus with that measured in the RF apparatus lends confidence to the measured yields.

This study provides a comprehensive measurement of k_1 and the first report of the direct determination of the products of reaction 1. However, the previous conclusion regarding the negligible contribution of reaction 1 to the lower stratospheric destruction of $ClONO_2$ remains unchanged. As noted in earlier papers, reaction 1 becomes a significant loss process only at higher altitudes, where the abundance of $ClONO_2$ is rather low.

Acknowledgment. We thank L. G. Huey for the CIMS analyses of the $ClONO_2$ samples, R. K. Talukdar for instructive discussion, and M. K. Gilles for help in synthesizing $ClONO_2$. This work was funded in part from the National Aeronautic and Space Administration's Mission to Planet Earth. L.G. thanks the NASA Global Change Research Program for a doctoral fellowship, and M.H.H. acknowledges a CIRES Visitor fellowship.

References and Notes

(1) Yokelson, R. J.; Burkholder, J. B.; Fox, R. W.; Talukdar, R. K.; Ravishankara, A. R. *J. Phys. Chem.* **1994**, *98*, 13144.
(2) Burkholder, J. B.; Talukdar, R. K.; Ravishankara, A. R. *Geophys. Res. Lett.* **1994**, *21*, 585−588.
(3) Hanson, D. R.; Ravishankara, A. R. *J. Geophys. Res.* **1991**, *96*, 5081−5090.
(4) Hanson, D. R.; Ravishankara, A. R. *J. Geophys. Res.* **1991**, *96*, 17307−17314.
(5) Yokelson, R. J.; Burkholder, J. B.; Goldfarb, L.; Fox, R. W.; Gilles, M. K.; Ravishankara, A. R. *J. Phys. Chem.* **1995**, *99*, 13976−13983.
(6) Yokelson, R. L.; Burkholder, J. B.; Ravishankara, A. R. *J. Phys. Chem.* **1997**, *101*, 6667−6678.
(7) Goldfarb, L.; Schmoltner, A.-M.; Gilles, M. K.; Burkholder, J. B.; Ravishankara, A. R. *J. Phys. Chem.* **1997**, *101*, 6658−6666.
(8) DeMore, W. B.; Sander, S. P.; Golden, D. M.; Hampson, R. F.; Kurylo, M. J.; Howard, C. J.; Ravishankara, A. R.; Kolb, C. E.; Molina, M. J. *Chemical Kinetics and Photochemical Data for Use in Stratospheric Modeling, Evaluation No. 12*; Jet Propulsion Laboratory: Pasadena, Calif., 1997.
(9) Molina, L. T.; Spencer, J. E.; Molina, M. J. *Chem. Phys. Lett.* **1977**, *45*, 158−162.
(10) Kurylo, M. J. *Chem. Phys. Lett.* **1977**, *49*, 467−470.
(11) Adler-Golden, S. M.; Wiesenfeld, J. R. *Chem. Phys. Lett.* **1981**, *82*, 281−284.
(12) Smith, W. S.; Chou, C. C.; Rowland, F. S. *Geophys. Res. Lett.* **1977**, *4*, 517−519.
(13) Vaghjiani, G. L.; Ravishankara, A. R. *Int. J. Chem. Kinet.* **1990**, *22*, 351−358.
(14) Schmeisser, M. Chlorine Nitrate. In *Handbook of Preparative Inorganic Chemistry*; Brauer, G., Ed.; Academic: San Diego, CA, 1967; p 326.
(15) Orkin, V. L.; Huie, R. E.; Kurylo, M. J. *J. Phys. Chem.* **1996**, *100*, 8907−8912.
(16) Moore, T. A.; Okumura, M.; Tagawa, M.; Minton, T. K. *Faraday Discuss. Chem. Soc.* **1995**, *100*, 295−307.
(17) Tyndall, G. S.; Kegley-Owen, C. S.; Orlando, J. J.; Calvert, J. G. *J. Chem. Soc., Faraday Trans.* **1997**, *93*, 2675.
(18) Malleson, A. M.; Kellet, H. M.; Myhill, R. G.; Sweetenham, W. P. *FACSIMILE*, version 4.0; AEA Technology, Harwell: Oxfordshire, U.K., 1995.
(19) Molina, L. T.; Molina, M. J. *J. Geophys. Res.* **1986**, *91*, 14501−14508.
(20) Harwood, M. H.; Jones, R. L.; Cox, R. A.; Lutman, E.; Rattigan, O. V. *J. Photochem. Photobiol.* **1993**, *A73*, 167−175.
(21) Harwood, M. H.; Burkholder, J. B.; Ravishankara, A. R. *J. Phys. Chem.* **1998**, *102*, 1309−1317.
(22) Ravishankara, A. R.; Davis, D. D.; Smith, G.; Tesi, G.; Spencer, J. *Geophys. Res. Lett.* **1978**, *4*, 7−9.
(23) Ravishankara, A. R.; Smith, G.; Watson, R. T.; Davis, D. D. *J. Phys. Chem.* **1977**, *81*, 2220−2225.
(24) Mauldin, R. L., III; Burkholder, J. B.; Ravishankara, A. R. *J. Phys. Chem.* **1992**, *96*, 2582−2588.
(25) Atkinson, R.; Baulch, D. L.; Cox, R. A.; Hampson, R. F.; Kerr, J. A.; Troe, J. *J. Phys. Chem. Ref. Data* **1992**, *21*, 1125−1568.